Density anomaly and liquid-liquid transition from perturbation theories

Jose B. Caballero and Antonio M. Puertas
Group of Complex Fluids Physics, Department of Applied Physics, University of Almeria, 04120 Almeria, Spain
(Received 4 August 2006; published 22 November 2006)

We report on theoretical results concerning the relation between the liquid-liquid transition and the density anomaly for a family of ramp potentials (hard-core plus linear short range repulsion and linear long range attraction). Using first order perturbation, we have studied the influence of the range of the attractive interactions, taking the repulsive part of the interaction as the reference system. Two different mechanisms of liquid-liquid coexistence have been predicted: attraction and compression. The attractive case is attributed to long ranged potentials, while the second one is obtained when the interaction is shortened. The density anomaly appears linked to regions where the temperature derivative of the density derivative of the energy is bigger (in absolute value) than a limit. This condition is fulfilled when the range of the attractive part of the potential is short enough.

DOI: 10.1103/PhysRevE.74.051506 PACS number(s): 64.70.Ja, 61.20.−p, 05.20.Jj

I. INTRODUCTION

It is generally accepted that liquid-liquid transitions are obtained in systems with two typical length scales in the interaction potential, supplemented by long-range attractive interactions [1]. These distances may arise due to orientation-dependent interactions, as for many atomic and molecular systems [2–7], or in spherically symmetric potentials [8–10]. Among the former, the paradigmatic example is water [3,4], not only because of its implications but also because it has eluded rationalization of its many anomalies; in particular, let us emphasize the density anomaly, i.e., the density increases upon cooling for a range of temperature and pressure. Different hypothesis have been developed [11,12], and although no compelling evidence for a liquid-liquid transition in supercooled water has been reported yet, there exist a variety of indirect experimental and theoretical data favoring the proposition that this transition exists in water and is the cause for the density anomaly [13–15].

For spherically symmetric potentials showing liquid-liquid separation, the core-softened or shoulder potentials introduced by Hemmer and Stell [16] are the most widely used examples, where the particle core exhibits a region of negative curvature or a step, in addition to a long range attraction. In these cases, however, the density anomaly is not always observed; see, e.g., Refs. [17–19] for nondifferentiable potentials which do not show it, or Refs. [8,9,20] for ramp potentials which indeed present density anomaly. In addition, purely repulsive core-softened potentials show density anomaly (as well as other thermodynamic and dynamic anomalies) without direct evidence of liquid-liquid phase separation, though there are indications that such a transition may exist but is preempted by crystallization (as it is speculated in the case of water) [21–24]. A rich scenario of crystal phases has also been predicted for convex repulsive potentials [25,26].

The first work for ramp potentials (hard core plus a repulsive linear potential at short distances, and linear attraction of longer range) studying the liquid-liquid coexistence accompanied by density anomaly was reported by Jagla [8], using computer simulations. This study, though, was restricted to one set of values for the hard-core diameter, soft-core diameter, and attraction range. Subsequently, this work was extended with more extensive simulations [9], confirming previous results, exactly locating the critical point and comparing its behavior with other shoulder potentials. More recently, a systematic computational study of this potential was performed by Gibson and Wilding [20], varying all the attraction range, repulsive range, and potential minimum. They found liquid-liquid separation, accompanied by density anomalies for all the cases they studied.

In this work, we use perturbation theory to study the relation between the liquid-liquid coexistence, the density anomaly, and the range of the attractive interaction for a family of ramp potentials with the functional form introduced by Jagla [8]. As reference system for the perturbation scheme we take (i) the standard hard-spheres system and (ii) the repulsive part of the total interaction potential. Note that for the latter the reference system already presents the density anomaly, which is absent in the former case [22,24]. The phase behavior is thus obtained using the variation of the energy with the density, what depends strongly on the temperature and the interaction potential. We identify two mechanisms to produce liquid-liquid transition: attraction for long ranged attractions and compression when the attractive interaction is shortened. With respect to the density anomaly, we show that it is related to regions where the temperature derivative of the density derivative of the energy is negative and smaller than a certain limit. Short ranged attractive potentials fulfill such a condition, but not long ranged ones.

The paper is organized as follows: in Sec. II the ramp potential and the methods are described. The results are presented in Sec. III, where they are also discussed. Finally, we outline the main conclusions in Sec. IV.

II. MODEL AND METHOD

The ramp potential introduced by Jagla consists of a hard core of diameter σ, a linear soft core, of diameter r_1, and a long range linear attraction, of range r_2 [8]. These three parts are connected to yield a continuous (nondifferentiable) potential:

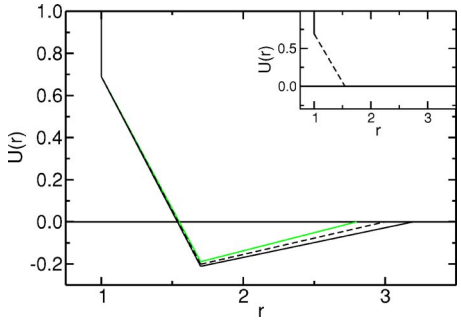

FIG. 1. (Color online) Ramp potential considered in this work where $\sigma=1$, $\epsilon=1$, $\gamma=0.31$, and $r_1=1.72$ have been fixed: $r_2=3.2$ (black line), $r_2=3$ (dashed line), and $r_2=2.8$ (grey line). Inset: repulsive reference system used in the MFOPT (see below) for $r_2=3$.

$$U(r)=\begin{cases}\infty, & r\le\sigma\\ \epsilon\left(\dfrac{r_1-r}{r_1-\sigma}\right)-\gamma\left(\dfrac{r_2-r}{r_2-\sigma}\right), & \sigma<r<r_1\\ -\gamma\left(\dfrac{r_2-r}{r_2-\sigma}\right), & r_1<r<r_2\\ 0, & r>r_2.\end{cases} \tag{1}$$

We will set $\epsilon=1$, $\sigma=1$, $\gamma=0.31$, and $r_1=1.72$. Three different r_2 values have been studied (Fig. 1): (i) $r_2=2.8$; (ii) $r_2=3$ (this system has been widely studied by computer simulations [8,9]); and (iii) $r_2=3.2$. The main difference between the potentials lies in the range of the attractive interaction, while a minor effect is observed in the repulsive part (see Fig. 1).

In first order perturbation theory (FOPT) the interaction potential is split up into two parts: $U(r)=U_0(r)+U_1(r)$; the reference system $[U_0(r)]$ plus a small perturbation term $[U_1(r)]$. Up to first order, the density Helmholtz free energy [i.e., $f(\rho,T)=F(\rho,T)/V$] in a thermodynamic state is estimated as [27]

$$f(\rho,T)=f_0(\rho,T)+\rho\langle u_1\rangle_0, \tag{2}$$

where f_0 is the density free energy of the reference system and $\langle u_1\rangle_0$ is the perturbation energy per particle averaged in the reference ensemble ($\langle u_1\rangle_0=2\pi\rho\int g_0(r)U_1(r)r^2dr$; here $g_0(r)$ is the radial distribution function of the reference system). Once $f(\rho,T)$ is known, the equation of state stems from

$$P=-f(\rho,T)+\rho\left(\frac{\partial f}{\partial\rho}\right)_T. \tag{3}$$

Usually, the hard-sphere fluid is taken as reference system, and the Carnahan-Starling equation of state is used [28]. The radial distribution function needed to compute the second term in Eq. (2) can be obtained from liquid state theory or computer simulations [27,29]. In this work, we have performed Monte Carlo simulations, as described below, to calculate $g_{HS}(r)$ and thus $\langle u_1\rangle_0$.

Under this approximation, while the entropy is approximated by the hard-sphere system, the calculation of the energy is based on the density modulations around the hard-core diameter σ. However core-softened fluids have two different typical lengths [1,18,20]. At high temperatures, where the energetic contributions are negligible, the characteristic distance is indeed the diameter of the particles. However, at low temperatures the pressure fixes the mean distance: σ for high pressures and r_1 at low ones. Because this fact is not considered within standard FOPT, we propose to use a different reference system to account for it.

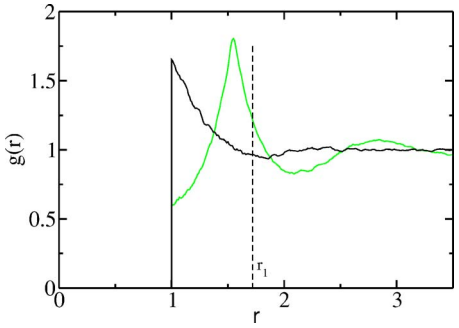

FIG. 2. (Color online) Pair distribution functions at $\rho=0.35$ for the hard spheres system (black line) and the repulsive part of the total potential at $T=0.2$ (grey line). Note the very different position of the first neighbors peak. The dashed line indicates r_1.

Since strictly repulsive ramp potentials present two typical distances [24], we have used the repulsive part of the interaction potential given in Eq. (1) as the reference system (see inset in Fig. 1). This system has been extensively studied by means of computer simulations [21], showing density anomaly. The new density free energy is thus

$$f(\rho,T)=f_{rep}(\rho,T)+\rho\langle u_{atr}\rangle_{rep}. \tag{4}$$

Now the attractive energy is computed by the density modulations around σ and r_1, with the pair distribution function $g_{rep}(r)$ calculated by Monte Carlo simulations. Figure 2 represents both distribution functions; contrary to $g_{HS}(r)$, $g_{rep}(r)$ shows the nearest neighbor peak at a distance between σ and r_1.

In Eq. (4) the free energy of the reference system is not known. It can be estimated, nevertheless, using perturbation theory in the standard way, that is, hard spheres is the reference system:

$$f_{rep}(\rho,T)=f_{HS}(\rho,T)+\rho\langle u_{rep}\rangle_{HS}. \tag{5}$$

In this approximation, $\langle u_{rep}\rangle_{HS}$ still uses the density modulations around σ, as given by the hard-spheres system. Thereby, we have approximated $\langle u_{rep}\rangle\approx\langle u_{rep}\rangle_{rep}$, and hence the total density free energy is

$$f(\rho,T)=f_{HS}(\rho,T)+\rho\langle u_{total}\rangle_{rep}. \tag{6}$$

Combining Eqs. (3) and (6),

$$P=P_{HS}+\rho^2\frac{\partial\langle u_{total}\rangle_{rep}}{\partial\rho}. \tag{7}$$

The pressure contains a volume exclusion term and an energetic contribution: the density derivative of the energy. The second term takes into account the density modulations around an average distance separating the particles, which

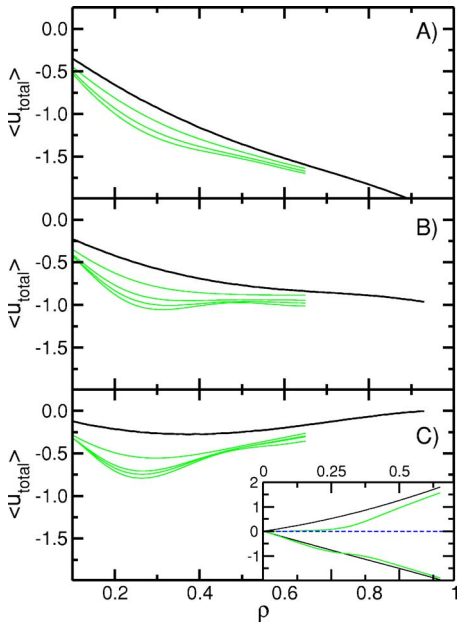

FIG. 3. (Color online) $\langle u_{total}\rangle_{rep}$ for the three systems studied (grey lines): (A) $r_2=3.2$ for $T=0.5$, 0.21, and 0.15 (from top to bottom); (B) $r_2=3$ for $T=0.35$, 0.15, 0.1, and 0.07 (from top to bottom) and (C) $r_2=2.8$ for $T=0.3$, 0.1, 0.08, and 0.06 (from top to bottom). $\langle u_{total}\rangle_{HS}$ is represented with black lines. Inset: attractive and repulsive contributions for $r_2=2.8$ at the hard-sphere limit (black lines) and $T=0.08$ (grey lines).

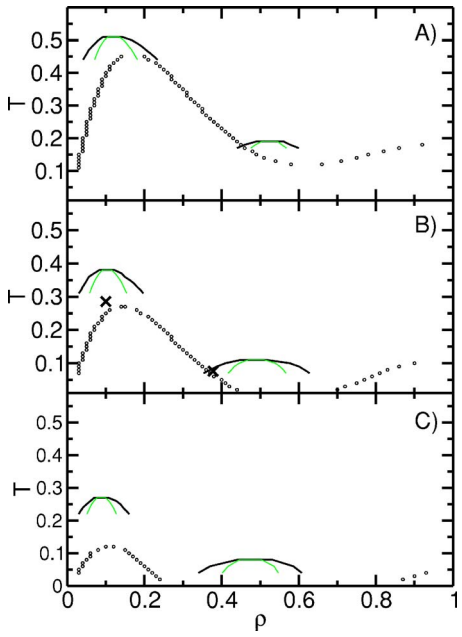

FIG. 4. (Color online) Binodals (black lines) and spinodals (grey lines) in the T-ρ plane using MFOPT: (A) $r_2=3.2$; (B) $r_2=3.0$ where crosses are the results from simulations [9]; and (C) $r_2=2.8$. Open circles: spinodals from FOPT with hard-sphere system as reference system (only spinodals are represented for clarity, since hard-spheres crystallization prevents calculations for the denser liquids).

depends on the thermodynamic state. This modified first order perturbation theory will be termed MFOPT.

To calculate the pair distribution functions, *NVT* Monte Carlo simulations with 512 particles were used for both reference systems. Each simulation comprised 20 000 cycles, half of them used to compute the pair distribution function. To evaluate the pressure, simulations at constant temperature were performed along the densities where the reference systems do not crystallize (up to $\rho=0.94$ in standard FOPT and $\rho=0.65$ for MFOPT). Once $\langle u_{total}\rangle_{rep}$ has been obtained, the isotherm is easily drawn from Eq. (7).

III. RESULTS

The systems under study present two critical points, one at low density and moderate temperature and another one at high density and low temperature. The former separates a dilute fluid from a dense one, i.e., liquid-gas transition, whereas in the latter two dense fluids are in coexistence, i.e., liquid-liquid coexistence, and will be studied in detail in the first subsection. In the second one, we will study if the density anomaly is present for any of the systems, and will analyze its origin.

A. Liquid-liquid coexistence

Figure 3 shows $\langle u_{total}\rangle_{HS}$ and $\langle u_{total}\rangle_{rep}$ as a function of density for the three sets of parameters investigated in this work. Under standard FOPT, $\langle u_{total}\rangle_{HS}$ does not depend on the temperature since $g(r)$ for hard-sphere fluids is a function exclusively of the density. On the other hand, MFOPT produces temperature dependent energy.

For all interaction ranges, at high temperatures the energy tends to the standard-FOPT result, as the only characteristic distance of the interaction potential is the hard-core diameter. At low temperatures, however, the core details, i.e., the repulsive ramp, affects the energy of the system. For low density values, the particles cannot penetrate into the repulsive part of the potential, and then, only attractive interactions are present. Upon increasing the density, at constant temperature, more pairs of particles come closer than r_1, which means that attractive and repulsive interactions are now involved; both contributions thus compete at high density and may result in a nonmonotonous behavior of the energy. Therefore we can see this phenomenon as an effective variation of the interaction potential which is enough to cause liquid-liquid phase separation [30].

As shown Fig. 3, for long range attractions the energy is a decreasing function of the density, at least in the temperature range investigated, with two inflexion points. For shorter interaction ranges, on the other hand, the energy presents a minimum at low temperatures and, again, two inflexion points. For $r_2=3.2$, the attractive contribution is larger than the repulsive one for the temperatures studied, resulting in a continuous decrease of the energy; for shorter interaction ranges, however, both contributions are comparable producing the minimum.

Once $\langle u_{total}\rangle_{rep}$ is known, using Eq. (7) the gas-liquid and liquid-liquid coexistence curves were obtained, see Fig. 4. In this plot, we also depict the spinodal from standard FOPT.

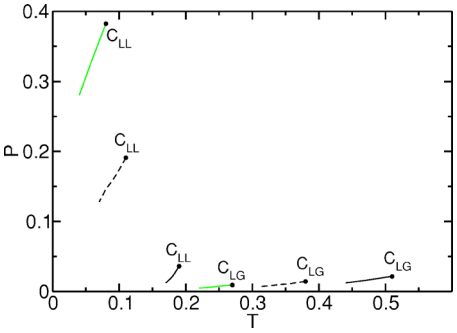

FIG. 5. (Color online) P-T projection of the phase diagram of the ramp potentials studied in this work: $r_2=3.2$ (black lines); $r_2=3.0$ (dashed lines); and $r_2=2.8$ (grey lines). Black circles represent critical points: C_{LG} liquid-gas critical points and C_{LL} liquid-liquid critical points.

The liquid-liquid transition is present for all values of r_2 under both approximations, arising from the variation of the effective interaction potential with the density [30]. However, the critical densities for both transitions are displaced to larger values in FOPT as compared with MFOPT, since higher pressure is needed to produce the density modulations around σ. As observed in Fig. 3, at high temperatures both approximations yield comparable results, but major differences are observed at low temperatures and high density, i.e., in the region where the liquid-liquid transition takes place. In addition to the theoretical results, the critical points for the system with $r_2=3.0$ from simulations are included, as estimated by Wilding and Magee [9]. Moderate agreement can be claimed for MFOPT, whereas the FOPT prediction for the liquid-liquid transition is completely wrong.

Next, we show the phase diagram in the P-T plane, see Fig. 5. It can be observed that the critical temperatures, both the gas-liquid and liquid-liquid ones, decrease as the range of the interaction is shortened. Interestingly, the critical pressure of the gas-liquid transition decreases slightly with decreasing r_2, while the pressure for liquid-liquid coexistence increases strongly. We interpret this phenomenon considering the energy curves (Fig. 3). For $r_2=3.2$, the longest interaction range studied in this work, the liquid-liquid separation is driven by the energy gained by the denser liquid, since the energy is always a decreasing function of the density at high and low temperatures. The situation changes for $r_2=3$ and $r_2=2.8$; here there exist density regions where the energy is an increasing function of ρ. Therefore the mechanism driving the transition is not energy but compression, i.e., at high density the particles try to be far away from each other because they do not gain energy in getting closer, increasing the density elsewhere in the system. Now the less dense liquid is favored energetically. Similar trends of the critical parameters of both transitions were obtained by Skibinsky *et al.* with a potential comprised by a repulsive step plus an attractive square well at longer distances [18].

The liquid-liquid transition has been discussed previously with different models. On one hand, such a transition was studied considering an effective diameter which changes with the state point $[\sigma=\sigma(\rho,T)]$ [18]. In this approximation, the energy term does not depend on temperature. On the other hand, the liquid-liquid coexistence was discussed by the variation of the interaction potential with the density [30]. Both approximations indeed reproduce the liquid-liquid coexistence. In contrast, in our approximation the theory takes into account the modulations around an average distance between the particles. That distance varies with the density and temperature, provoking the change of the effective interaction potential with the density and producing energy curves which depend on T (see Fig. 3). It is interesting to note that in our case, the phenomenology arises from an energetic description of the system, presenting a clear relation between the microscopic interactions and the macroscopic behavior.

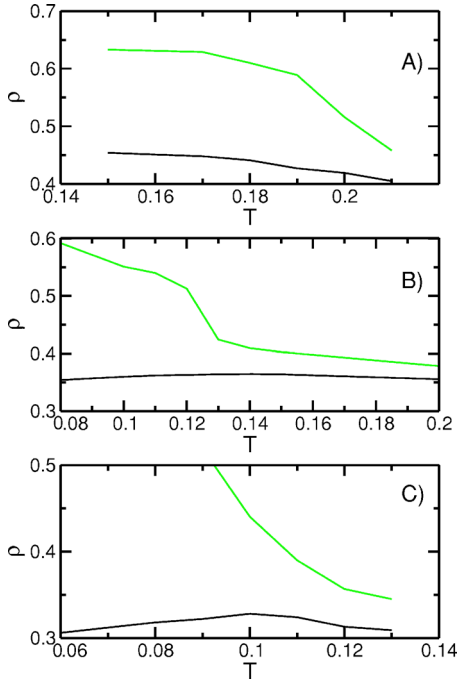

FIG. 6. (Color online) Density vs T at fixed pressure (indicated in each case): (A) $r_2=3.2$ for $P=0.015$ (black line) and $P=0.05$ (grey line); (B) $r_2=3$ for $P=0.12$ (black line) and $P=0.2$ (grey line); and (C) $r_2=2.8$ for $P=0.2$ (black line) and $P=0.4$ (grey line).

B. Density anomaly

Computer simulations confirmed that the ramp potential presents a density anomaly for a wide range of parameters [8,9,20], including the case $r_2=3$, explicitly studied in Ref. [9]. The increase of the density with temperature was found for supercritical temperatures and critical to subcritical pressures (with respect to the liquid-liquid transition). The standard FOPT, though, does not find any density anomaly in this region. However, we indeed find a density anomaly using MFOPT for $r_2=2.8$ and $r_2=3$, but not for $r_2=3.2$, as shown in Fig. 6. Note that the thermodynamic anomaly appears in the region located between gas-liquid and liquid-liquid transitions (in agreement with the simulations), but disappears at supercritical pressures (grey lines in Fig. 6).

In the following, we address two points arising from these results: (i) why FOPT cannot predict the density anomaly

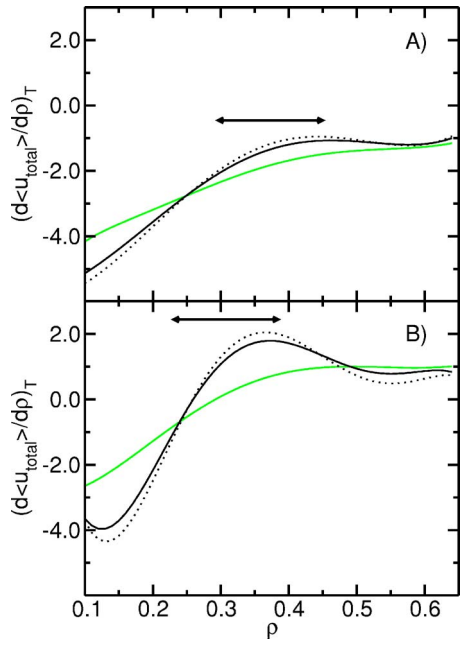

FIG. 7. (Color online) Density derivative of the total energy $\langle u_{total}\rangle$: (A) $r_2=3.2$ for $T=0.5$ (grey line), $T=0.21$ (black line), and $T=0.15$ (dashed line); and (B) $r_2=2.8$ for $T=0.3$ (grey line), $T=0.08$ (black line), and $T=0.06$ (dashed line). The arrows indicate the density regions where $\left[\frac{\partial}{\partial T}\left(\frac{\partial\langle u\rangle}{\partial\rho}\right)_T\right]_\rho<0$.

and (ii) why the system with $r_2=3.2$ does not have a density anomaly.

The density anomaly is given by $\left(\frac{\partial V}{\partial T}\right)_P<0$, using Maxwell relations

$$\left(\frac{\partial V}{\partial T}\right)_P=-\left(\frac{\partial S}{\partial P}\right)_T=-\left(\frac{\partial S}{\partial V}\right)_T\left(\frac{\partial V}{\partial P}\right)_T<0. \tag{8}$$

For stable phases $\left(\frac{\partial V}{\partial P}\right)_T<0$. Thus having a density anomaly implies

$$\left(\frac{\partial S}{\partial V}\right)_T=\left(\frac{\partial P}{\partial T}\right)_V<0. \tag{9}$$

Applying this condition to Eq. (7),

$$\left(\frac{\partial P_{HS}}{\partial T}\right)_V+\rho^2\left[\frac{\partial}{\partial T}\left(\frac{\partial\langle u_{total}\rangle_{rep}}{\partial\rho}\right)_T\right]_V<0. \tag{10}$$

Note that the first term is strictly positive; i.e., $\left(\frac{\partial P_{HS}}{\partial T}\right)_V>0$. Thus the second term must be negative and bigger (in absolute value) than the first one. It is now clear why FOPT cannot produce any density anomaly: $\langle u_{total}\rangle_{HS}$ does not depend on T and thus the second term of the expression above is zero.

The disappearance of the density anomaly for $r_2=3.2$ can also be rationalized using this expression. In Fig. 7, the density derivative of the energy is presented for different temperatures, for the system with $r_2=3.2$ (upper panel) and $r_2=2.8$ (lower panel). In both cases, the second term in Eq. (10) is negative for a range of densities, marked by the arrows. However, the density anomaly does not appear for $r_2=3.2$ because in this case the energy varies too slowly with temperature, and its derivative is not large enough to overcome the hard-sphere contribution. In contrast, the variation of $\left(\frac{\partial\langle u\rangle}{\partial\rho}\right)_T$ vs T for $r_2=2.8$ (and $r_2=3.0$) is stronger, and the system presents the density anomaly. Noteworthy is that the density anomalies appear associated to systems with liquid-liquid separation driven by compression, since for these systems the energy depends strongly on T (see Fig. 3). For $r_2=3.2$, on the other hand, the system gains energy when the density is increased what produces a weak dependence of the energy on temperature.

Therefore the presence of a density anomaly depends on both r_1 and r_2, i.e., it is not only set by the repulsive interactions, as was already shown for purely repulsive systems [24]. When the system is dominated by the attractive interactions, that is, the energy is always a decreasing function of the density (in our case, the system with $r_2=3.2$), the system can possess two critical points but no density anomaly. On the contrary, the system with a liquid-liquid transition driven by compression can have a density anomaly, associated to regions where the energy is an increasing function of the density.

IV. CONCLUSIONS

We have shown the predictions from perturbation theory for a family of ramp potentials, using as a reference system hard spheres and the repulsive part of the total interaction potential. The latter accounts for the density modulations around a typical distance which depends on the density and temperature, and which varies between the soft-core diameter and the hard-core one. The use of this reference system improves the results of the theory regarding the liquid-liquid coexistence, and is necessary in order to predict the density anomaly.

Two different mechanisms of liquid-liquid coexistence have been found for these potentials: (i) attraction driven, when the energy is a decreasing function of the density for all the temperatures (for long ranged attractive interactions), and (ii) compression driven, characterized by a region where the energy increases with the density. The density anomaly appears linked to regions where the temperature derivative of the density derivative of the energy is negative and smaller than a limit. Such a condition is fulfilled when the attractive part of the interaction has a short enough range.

ACKNOWLEDGMENTS

We thank M. E. Cates and N. B. Wilding for useful discussions. This work was financially supported by the Ministerio de Educación y Ciencia, under Project No. MAT2004-03581.

[1] G. Franzese, G. Malescio, A. Skibinsky, S. V. Buldyrev, and H. E. Stanley, Nature (London) **409**, 691 (2001).
[2] P. G. Debenedetti, *Metastable Liquids: Concepts and Principles* (Princeton University Press, Princeton, NJ, 1998).
[3] O. Mishima and H. E. Stanley, Nature (London) **396**, 329 (1998).
[4] C. A. Angell, Annu. Rev. Phys. Chem. **55**, 559 (2004).
[5] Y. Katayama, T. Mizutani, W. Utsumi, O. Shimomura, M. Yamakata, and K. Funakoshi, Nature (London) **403**, 170 (2000).
[6] Y. Katayama, Y. Inamura, T. Mizutani, M. Yamakata, W. Utsumi, and O. Shimonura, Science **306**, 848 (2004).
[7] R. Kurita and H. Tanaka, Science **306**, 845 (2004).
[8] E. A. Jagla, Phys. Rev. E **63**, 061501 (2001).
[9] N. B. Wilding and J. E. Magee, Phys. Rev. E **66**, 031509 (2002).
[10] L. Xu, P. Kumar, S. V. Buldyrev, S.-H. Chen, P. H. Poole, F. Sciortino, and H. E. Stanley, Proc. Natl. Acad. Sci. U.S.A. **102**, 16558 (2005).
[11] R. J. Speedy, J. Chem. Phys. **86**, 982 (1982).
[12] P. H. Poole, F. Sciortino, U. Essmann, and H. E. Stanley, Nature (London) **360**, 324 (1992).
[13] O. Mishima, Phys. Rev. Lett. **85**, 334 (2000).
[14] M. Yamada, S. Mossa, H. E. Stanley, and F. Sciortino, Phys. Rev. Lett. **88**, 195701 (2002).
[15] N. Giovambattista, H. E. Stanley, and F. Sciortino, Phys. Rev. Lett. **94**, 107803 (2005).
[16] P. C. Hemmer and G. Stell, Phys. Rev. Lett. **24**, 1284 (1970); G. Stell and P. C. Hemmer, J. Chem. Phys. **56**, 4274 (1972).
[17] G. Franzese, G. Malescio, A. Skibinsky, S. V. Buldyrev, and H. E. Stanley, Phys. Rev. E **66**, 051206 (2002).
[18] A. Skibinsky, S. V. Buldyrev, G. Franzese, G. Malescio, and H. E. Stanley, Phys. Rev. E **69**, 061206 (2004).
[19] G. Malescio, G. Franzese, A. Skibinsky, S. V. Buldyrev, and H. E. Stanley, Phys. Rev. E **71**, 061504 (2005).
[20] H. M. Gibson and N. B. Wilding, Phys. Rev. E **73**, 061507 (2006).
[21] P. Kumar, S. V. Buldyrev, F. Sciortino, E. Zaccarelli, and H. E. Stanley, Phys. Rev. E **72**, 021501 (2005).
[22] Z. Yan, S. V. Buldyrev, N. Giovambattista, and H. E. Stanley, Phys. Rev. Lett. **95**, 130604 (2005).
[23] A. Barros de Oliveira, P. A. Netz, T. Colla, and M. C. Barbosa, J. Chem. Phys. **124**, 084505 (2006).
[24] Z. Yan, S. V. Buldyrev, N. Giovambattista, P. G. Debenedetti, and H. E. Stanley, Phys. Rev. E **73**, 051204 (2006).
[25] E. Velasco, L. Mederos, G. Navascués, P. C. Hemmer, and G. Stell, Phys. Rev. Lett. **85**, 122 (2000).
[26] P. C. Hemmer, L. Mederos, G. Navascués, E. Velasco, and G. Stell, J. Chem. Phys. **114**, 2268 (2001).
[27] J. P. Hansen and I. R. McDonald, *Theory of Simple Liquids* (Academic, San Diego, 1986).
[28] N. F. Carnahan and K. E. Starling, J. Chem. Phys. **51**, 635 (1969).
[29] D. Frenkel and B. Smit, *Understanding Molecular Simulations* (Academic, San Diego, 1996).
[30] N. G. Almarza, E. Lomba, G. Ruiz, and C. F. Tejero, Phys. Rev. Lett. **86**, 2038 (2001).